

The regulated elimination of transit-amplifying cells preserves tissue homeostasis during protein starvation in *Drosophila* testis

Heiko Yang¹ and Yukiko M. Yamashita^{1,2,3,*}

ABSTRACT

How tissues adapt to varying nutrient conditions is of fundamental importance for robust tissue homeostasis throughout the life of an organism, but the underlying mechanisms are poorly understood. Here, we show that *Drosophila* testis responds to protein starvation by eliminating transit-amplifying spermatogonia (SG) while maintaining a reduced pool of actively proliferating germline stem cells (GSCs). During protein starvation, SG die in a manner that is mediated by the apoptosis of somatic cyst cells (CCs) that encapsulate SG and regulate their development. Strikingly, GSCs cannot be maintained during protein starvation when CC-mediated SG death is inhibited, leading to an irreversible collapse of tissue homeostasis. We propose that the regulated elimination of transit-amplifying cells is essential to preserve stem cell function and tissue homeostasis during protein starvation.

KEY WORDS: *Drosophila*, Starvation, Stem cells, Transit-amplifying cells

INTRODUCTION

Tissue homeostasis, defined as the balanced state between cell production and loss, must change in response to nutrient conditions in order to optimize the efficient use of resources (Fielenbach and Antebi, 2008; Lopes et al., 2004; Tatar and Yin, 2001). Although it may be advantageous for tissues to robustly generate new cells when nutrients are abundant, proliferation must be scaled down when nutrients are limited or absent (Angelo and Van Gilst, 2009; Padilla and Ladage, 2012). Thus, to cope with the fluctuating availability of food throughout life, tissues often shift between different states of homeostasis. How such ‘shifting’ is accomplished is poorly explored, and little is known about how impairments in this process can irreversibly impact overall tissue organization and functionality. Considering that many human diseases, most notably those associated with aging and cancer, are characterized by dysfunctional tissue homeostasis, it is possible that defective ‘shifts’ in tissue homeostasis might underlie these pathological conditions. An understanding of such mechanisms could thus reveal previously unexplored strategies for therapy.

Because stem cells are responsible for generating new cells within a tissue, much of the attention in understanding tissue homeostasis has been focused on the their behavior (Mihaylova et al., 2014; Nakada et al., 2011). However, stem cells are likely not the only point of regulation. In many tissues, stem cells produce differentiating

daughters that undergo transit-amplifying divisions prior to terminal differentiation (Davies and Fuller, 2008; Lui et al., 2011; van der Flier and Clevers, 2009; Watt, 1998), which is thought to be a strategy to protect stem cells from exhaustion. Transit-amplifying cells represent a considerable fraction of cell divisions within many tissues and likely also contribute to shifting tissue homeostasis. Although it has been reported that nutrients can affect the behavior of transit-amplifying cells (Drummond-Barbosa and Spradling, 2001; Yilmaz et al., 2012), it remains unclear how the response of stem cells and transit-amplifying cells are integrated in a concerted manner to allow a tissue to adapt to fluctuating nutrient conditions.

The *Drosophila* testis is an ideal model system in which to investigate the behavior of stem cells and transit-amplifying cells. The system offers unequivocal identification of these cell types at the single cell resolution, allowing detailed examination of their behavior during different states of tissue homeostasis. Germ cell production begins at the apical tip, where germline stem cells (GSCs) reside in a well-defined niche organized by the somatic hub cells (Lehmann, 2012; Losick et al., 2011). GSCs give rise to spermatogonia (SG) that undergo transit amplification and differentiation with the support of somatic cyst cells (CCs) (de Cuevas and Matunis, 2011; Lim and Fuller, 2012; Schulz et al., 2002). In *Drosophila* male and female germ lines, gametogenesis is highly sensitive to the availability of dietary amino acids (Drummond-Barbosa and Spradling, 2001; McLeod et al., 2010; Roth et al., 2012; Wang et al., 2011). In the testis, germ cell production scales down during protein starvation, and the reduction of the germline is reflected by dramatic involution of the tissue. Importantly, the testis can efficiently recover and increase germ cell output when protein is reintroduced into the diet (McLeod et al., 2010). This system provides a simple yet powerful paradigm with which to investigate how tissue homeostasis shifts in response to changes in nutrient availability.

Here, we report that the *Drosophila* testis maintains a reduced pool of actively proliferating GSCs during prolonged protein starvation. The reduction in the overall production of germ cells is achieved by the elimination of transit-amplifying SG, which is triggered by the apoptosis of somatic CCs. We further show that the regulated elimination of SG is vital to ensuring GSC maintenance during starvation. Inhibition of SG death during protein starvation leads to GSC dysfunction and a collapse in tissue homeostasis, leading to a failure in recovery upon reintroduction of nutrients to the system. We propose that a coordinated response among multiple cell types within a tissue is essential for successfully shifting tissue homeostasis in response to changes in nutrient availability.

RESULTS

Stem cells are maintained in a steady state during prolonged protein starvation

It has previously been reported that in wild-type *Drosophila* testes, average germline stem cell (GSC) number decreases from

¹Life Sciences Institute, University of Michigan, Ann Arbor, MI 48109-2219, USA.

²Department of Cell and Developmental Biology, University of Michigan, Ann Arbor, MI 48109-2216, USA. ³Howard Hughes Medical Institute, University of Michigan, Ann Arbor, MI 48109-2216, USA.

*Author for correspondence (yukikom@umich.edu)

approximately eight to six per testis after 15 days of protein starvation (McLeod et al., 2010), which we confirmed using similar protein starvation conditions (Fig. 1A). During this time period, hub cell number, expression of the niche ligand *Upd* in the hub or expression of *Stat92E* in GSCs as a result of niche signaling did not noticeably change (supplementary material Fig. S1). Interestingly, we found that stem cell loss does not proceed linearly. GSC number decreased between day 3 and day 6 of protein starvation (Fig. 1A), but no further decrease was observed for at least 12 additional days. The fact that approximately six GSCs are maintained during prolonged starvation prompted us to investigate the manner in which GSCs are maintained.

To determine whether the six remaining GSCs become quiescent or have altered proliferation, we compared the cell cycle activity of GSCs in fed and starved conditions using several different experimental paradigms. We first measured the frequency of GSCs in S phase or in mitosis and found no difference between fed and starved conditions (supplementary material Fig. S2). To further validate these results, we examined the kinetics of BrdU incorporation in GSCs upon continuous BrdU feeding using flies that had been starved for 2, 9 and 18 days. After subjecting flies at

each time point to 48 h (equivalent to approximately three normal cell cycles) of continuous BrdU feeding, we expected three major possible outcomes: if all GSCs in the starved condition are indeed proliferating similarly to those in the age-matched fed controls (Fig. 1B, hypothetical scenario 1), all the GSCs will become BrdU⁺ at the same rate as in fed conditions; if all GSCs are proliferating but at a slower rate during starvation, all the GSCs will still become BrdU⁺ but at a later time point than those in fed conditions (Fig. 1B, hypothetical scenario 2); if a subset of GSCs becomes quiescent, the percentage of GSCs to become BrdU⁺ will plateau at less than 100% (Fig. 1B, hypothetical scenario 3). The results of continuous BrdU feeding shown in Fig. 1C reveal that GSCs transiently slow down after 2 days of starvation, but all GSCs proliferate at the same rate as those in fed conditions after 9 or 18 days of starvation (Fig. 1C). This suggests that the cell cycle length of GSCs is unaffected during prolonged protein starvation and that no GSCs become quiescent. Although it was previously suggested that a combination of decreased GSC number and decreased GSC cell cycle index leads to tissue involution during protein starvation (McLeod et al., 2010), our results instead indicate that the contribution of decreased GSC cell cycle is not significant. The

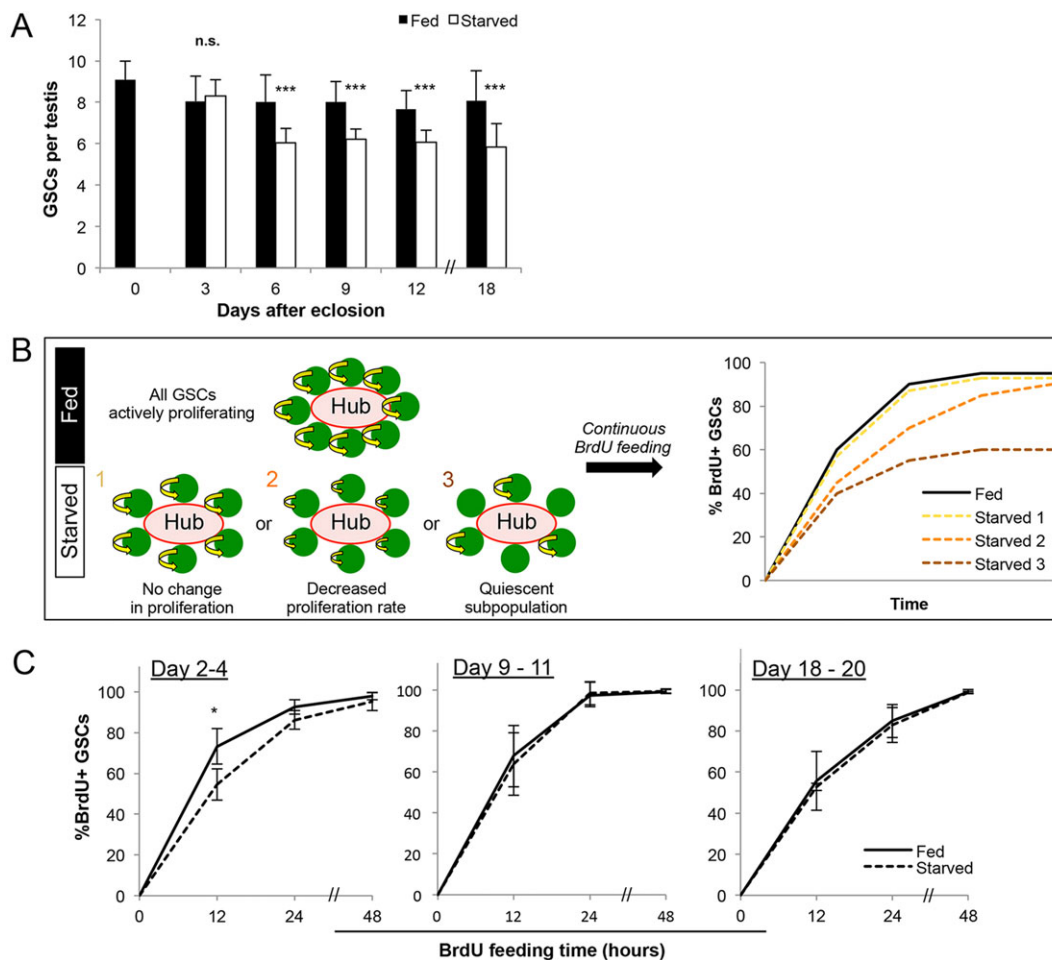


Fig. 1. GSCs are maintained at a reduced number and continue to proliferate during starvation. Wild-type (*yw*) flies that were allowed to develop to adulthood in a rich protein source were transferred into fed (protein rich) or starved conditions upon eclosion. (A) Average GSC number per testis over 18 days in fed versus starved conditions. Data are mean \pm s.d. $n > 30$ testes per data point. *** $P < 0.0005$ (Student's *t*-test). (B) Three hypothetical scenarios of GSC behavior during starvation tested by continuous BrdU feeding: (1) no change in proliferation, reflected by an equal rate of BrdU incorporation compared with fed control; (2) decreased overall proliferation, reflected by reduced BrdU incorporation kinetics; and (3) a quiescent subpopulation, in which some GSCs will never become positive for BrdU. (C) Kinetics of BrdU incorporation over 48 h beginning on days 2, 9 and 18. Data are mean \pm s.d. $n > 100 \times 3$ GSCs per data point. * $P < 0.05$ (Student's *t*-test).

decrease in cell cycle indices after 9 days in both fed and starved conditions likely reflects an effect of aging rather than starvation (Inaba et al., 2011).

We have previously reported that flies cultured in ‘poor’ media – containing low levels of protein as opposed to none in the protein starvation condition described in this study – have GSCs with high rates of centrosome misorientation with respect to the hub (Roth et al., 2012), which slows the cell cycle via the centrosome orientation checkpoint (Cheng et al., 2008). This is seemingly contradictory to our observation here that GSC cell cycle is unchanged during protein starvation. However, GSC number does not decrease in poor media (Roth et al., 2012), as opposed to the protein starvation condition, in which 25% (two out of eight) of GSCs are lost. Interestingly, on day 3 of protein starvation, which is prior to GSC loss (Fig. 1A), we observed a transient increase in centrosome misorientation (supplementary material Fig. S3A,B), concomitant with a transient decrease in cell cycle progression (Fig. 1C; supplementary material Fig. S3C). Following GSC loss between day 3 and day 6, GSC centrosome misorientation decreases and remains low, which is in a full agreement with McLeod et al. (2010) who reported no significant centrosome misorientation after 17 days of starvation. Thus, we speculate that, at the initial phase of protein starvation, the systemic environment transitions through a poor nutrient state in which GSC number is maintained but cell cycle is slowed. Upon reaching a steady state in protein starvation after 6 days of starvation, two out of eight GSCs are lost, and the remaining six GSCs have normal cell cycle activity. These results suggest that protein restriction and protein starvation present distinct challenges to which the system responds differently.

Transit-amplifying spermatogonia are eliminated during protein starvation

The presence of six active GSCs throughout prolonged protein starvation prompted us to ask whether a response in other cell types may also contribute to the dramatic involution of the testis during protein starvation as described previously (McLeod et al., 2010). We therefore turned our attention to the transit-amplifying cells, i.e. spermatogonia (SG). After each GSC division, the differentiating daughter cells, called the gonialblasts (GBs), undergo exactly four rounds of transit-amplifying divisions as SG prior to becoming spermatocytes. As in mammals, SG divisions are characterized by incomplete cytokinesis, yielding two-, four-, eight- and 16-cell SG. Each stage can be readily identified by counting the number of SG that are interconnected by branching fusomes (Lin et al., 1994). When SG were quantified according to stage, we found a specific decrease in the four-, eight- and 16-cell SG without a significant decrease in the number of GBs and two-cell SG under protein starvation conditions (Fig. 2A). These results suggest that transit-amplifying divisions are specifically impaired around the two- and four-cell stage in response to protein starvation.

We investigated the nature of SG reduction during protein starvation and found that SG death, particularly at the four-cell stage, was increased. As recently reported (Yacobi-Sharon et al., 2013), germ cell death occurs sporadically during normal spermatogenesis in a caspase 3-independent manner. Accordingly, dying germ cells cannot be identified using conventional markers of apoptosis, such as anti-cleaved caspase 3 staining or the apoptosis sensor Apoliner (Bardet et al., 2008) (see below). Instead, we detected dying germ cells using Lysotracker, which stains the acidified compartments associated with dying germ cells (Yacobi-Sharon et al., 2013). Yacobi-Sharon et al. reported that dying germ cells are positive for both Lysotracker and TUNEL, which was confirmed to be true

under starved conditions as well (supplementary material Fig. S4A). As TUNEL can stain both apoptotic somatic cells and dying germ cells, we used Lysotracker as a primary method to detect germ cell death. Using Lysotracker, we noticed that SG die more frequently during protein starvation. When we quantified SG death per testis relative to SG stage (Fig. 2B; supplementary material Fig. S4B-E), we found that GBs, two-cell SG and four-cell SG die more frequently compared with fed conditions after 3 days and 9 days of protein starvation (Fig. 2C). After 9 days of starvation, the increase in SG death was most prominent at the four-cell stage (Fig. 2C). The data collectively suggest that the cumulative increase in GB, two-cell and particularly four-cell SG death accounts for the decrease in late-stage SG (i.e. eight- and 16-cell SG stages) at day 9 and day 18 of protein starvation. The death of eight- and 16-cell SG does not appear to be affected by starvation, presumably because late-stage SG death is governed primarily by a nutrient-independent mechanism, as previously described (Yacobi-Sharon et al., 2013) (Fig. 2D). It should be noted that a subset of dying SG could not be categorized by stage due to lack of lamin staining (a marker required for identifying SG stage) at the very last phase of SG death (supplementary material Fig. S4E). These dying SG of unknown stage identity were not included in our stage-specific quantification of SG death.

These data indicate that the survival of SG in the early stages of transit-amplifying divisions is significantly impaired upon protein starvation. As we were unable to detect a significant change in the rate of SG divisions during starvation, assessed by the frequency of SG mitoses, we conclude that SG death is most likely responsible for decreased SG number.

Starvation increases the apoptosis of cyst cells

SG require supporting somatic CCs to undergo transit-amplifying divisions and differentiation (de Cuevas and Matunis, 2011; Lim and Fuller, 2012; Schulz et al., 2002). Their progenitors, called cyst stem cells (CySCs), are attached to the hub and provide essential signals to specify GSC identity (Leatherman and DiNardo, 2008, 2010). CySCs divide asymmetrically to produce CCs (Cheng et al., 2011), which encapsulate GBs/SG to promote their differentiation (Lim and Fuller, 2012; Schulz et al., 2002).

In parallel with the elimination of SG, the number of CCs marked by Tj (Li et al., 2003), but not cyst stem cells (CySCs) marked by Zfh1 (Leatherman and DiNardo, 2008), was notably decreased during protein starvation (Fig. 3A,B). Although it was reported that the number of CySCs decline after 20 days of protein starvation (McLeod et al., 2010), the difference is not yet dramatic after 9 days of protein starvation (Fig. 3B), when a decrease in the number of CCs (Zfh1⁻, Tj⁺) is already pronounced. Further investigation revealed that the decrease in CC number is due to CC apoptosis. CC death can be detected by Apoliner (Fig. 3C-F), a fluorescent reporter that yields nuclear localization of nlsGFP (henceforth described as ‘Apoliner⁺’) in the presence of activated caspases (Bardet et al., 2008). Consistent with the previous study by Bardet et al., anti-cleaved caspase 3 antibody staining was detected in Apoliner⁺ cells at late stages of cell death (Fig. 3E). We further found that the dying CCs were far from the hub and were almost never Zfh1⁺ (Fig. 3F), suggesting that CCs but not CySCs undergo apoptosis during starvation. By scoring Apoliner⁺ cells relative to the total number of CCs, we detected a twofold increase in CC apoptosis during protein starvation (Fig. 3G). Importantly, the frequency of CySC mitoses, which we measured using phospho-histone H3 staining, did not decrease significantly relative to GSC mitotic index (fed, 3.7±1.0 per dividing GSC; starved, 3.0±1.0 per dividing GSC; *n*>50×3 testes, *P*>0.05),

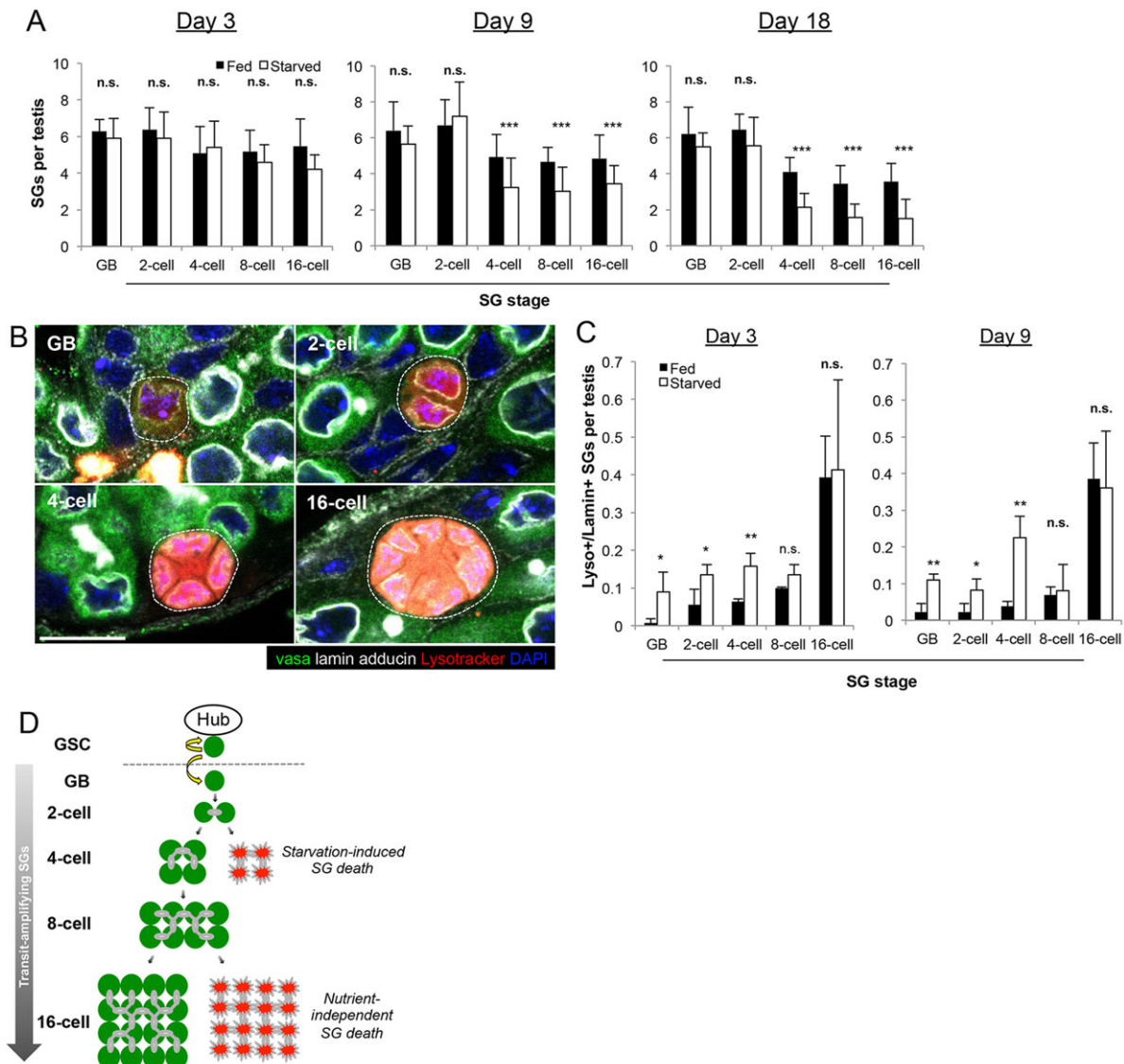


Fig. 2. Spermatogonia are eliminated around the two-cell and four-cell stages during protein starvation. (A) SG number per stage per testis at days 3, 9 and 18. The SG stage was determined by counting the number of SG connected by a fusome. Data are mean±s.d. $n>20$ testes per condition per time point. *** $P<0.0005$ (Student's *t*-test). (B) Representative images of dying SG (dotted outline) stained for lamin, which allows SG death to be scored according to stage as dying GBs, or two-, four-, eight- or 16-cell SG (some cells are not visible due to focal plane limitations). Scale bar: 10 μ m. (C) Quantification of SG death by stage on day 3 and day 9 of starvation. Data are mean±s.d. $n>30\times 3$ testes per data point. * $P<0.05$; ** $P<0.005$ (Student's *t*-test). (D) Schematic model of SG death.

Protein starvation increases SG death near the two-cell to four-cell transition, whereas death at the later stages occurs independently of nutrient conditions.

suggesting that the primary effect of starvation on the CySC/CCs is to increase CC apoptosis.

CC apoptosis mediates starvation-induced SG death

Because CCs play a crucial role during SG development (Lim and Fuller, 2012; Tazuke et al., 2002), we hypothesized that the increase in CC apoptosis during starvation mediates the increase in SG death. To explore this relationship, we first examined whether CC apoptosis was sufficient to trigger SG death. We induced CySC/CC apoptosis using temperature-dependent expression of the proapoptosis gene Grim in the CySC/CC lineage ($c587\text{-gal4}>UAS\text{-Grim}$, $tub\text{-gal80}^{ts}$), as previously described (Hétié et al., 2014; Lim and Fuller, 2012). Consistent with the reported observation that expression of Grim in the CySC/CC lineage ablates germ cells as well as CySCs/CCs, we observed a dramatic increase in SG death upon Grim induction (supplementary

material Fig. S5). We also noted that all SG death induced by the somatic expression of Grim is associated with LysoTracker and has morphological characteristics reminiscent of starvation-induced SG death. These results indicate that CC apoptosis is sufficient to initiate SG death rapidly and suggest that starvation-induced SG death follows a similar mechanism.

To test this idea further, we inhibited CC apoptosis during protein starvation using overexpression of *Drosophila* inhibitor of apoptosis 1 protein (DIAP1) (Orme and Meier, 2009), as well as knockdown of the initiator caspase Dronc with RNAi (Leulier et al., 2006). While these manipulations did not alter SG death under fed conditions, we found that inhibition of CC apoptosis led to a considerable decrease in starvation-induced CC apoptosis (Fig. 4A), which was accompanied by a significant decrease in SG death at the two- and four-cell SG stages (Fig. 4B). Importantly, knockdown of Dronc in germ cells ($nos>Dronc\text{-RNAi}$) did not suppress SG death

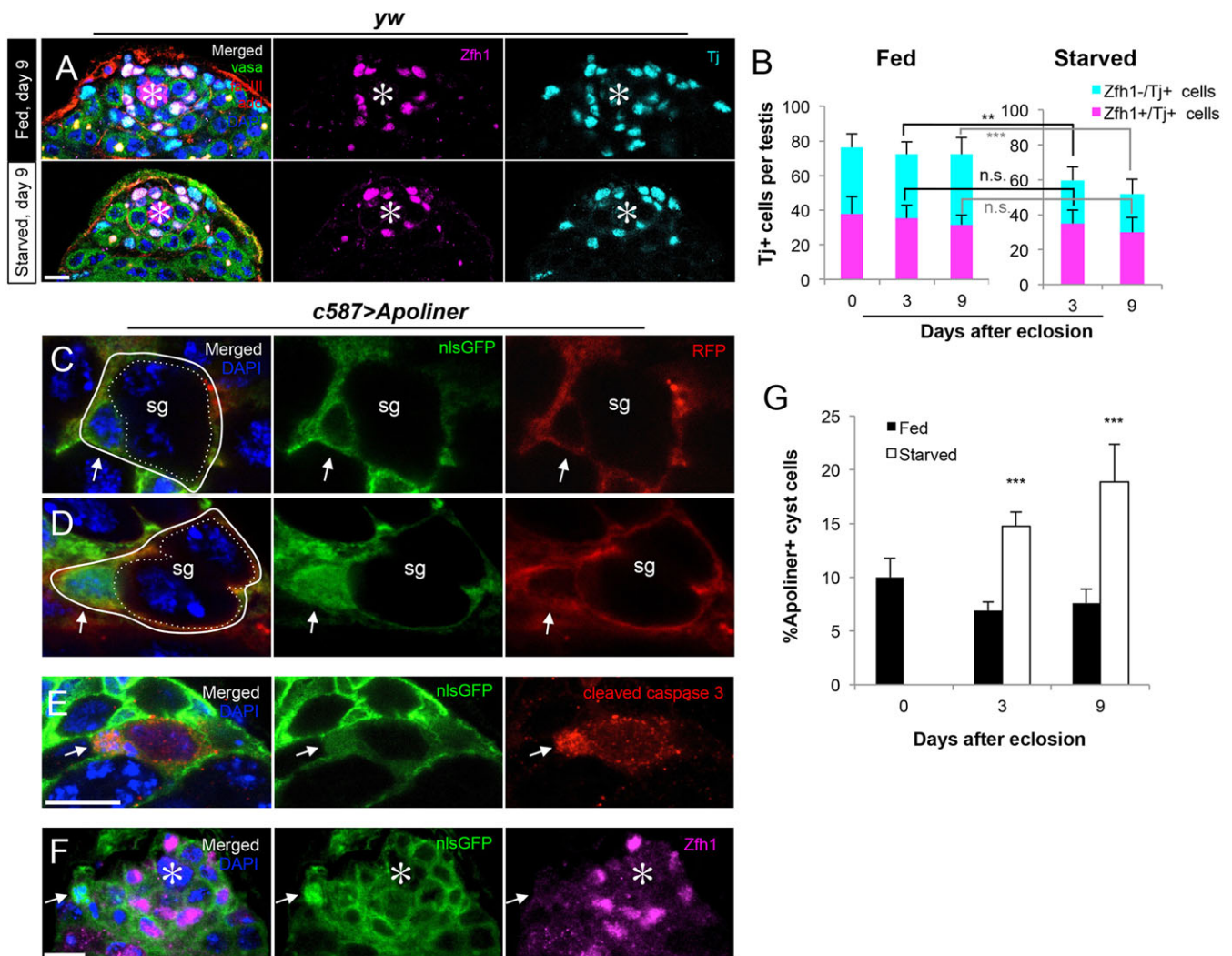


Fig. 3. Apoptosis of cyst cells increases during protein starvation. (A) Representative images of testes stained with the CySC marker Zfh1 and the CySC/CC marker Tj in fed versus starved conditions. (B) Quantification of Tj⁺ and Zfh1⁺ nuclei on days 0, 3 and 9. $n > 30$ testes per time point. Data are mean \pm s.d. $^{**}P < 0.005$; $^{***}P < 0.0005$ (Student's *t*-test). (C) An example of non-apoptotic CC (solid white outline) visualized by Apoliner. Apoliner was expressed in the CySC/CC lineage using the *c587-gal4* driver. A CC without nuclear GFP (arrow) encapsulates a two-cell SG (dotted outline). (D) An example of an Apoliner⁺ apoptotic CC (solid white outline) with a nlsGFP⁺ nucleus (arrows). mCD8-RFP is localized to the CC membrane in both scenarios. (E) An example of cleaved caspase 3 staining colocalizing with a dim Apoliner signal that is characteristic of later stages of apoptosis (arrows). (F) A representative image of an Apoliner⁺ cell (arrows), demonstrating that apoptotic CCs are always away from the hub (asterisks) and barely Zfh1⁺. (G) Frequency of Apoliner⁺ CCs scored as percentage of all Tj⁺/Zfh1⁻ cells. Data are mean \pm s.d. $n > 20 \times 3$ testes per condition per time point. $^{***}P < 0.0005$ (Student's *t*-test). Scale bars: 10 μ m.

(supplementary material Fig. S6), and it was previously reported that DIAP1 expression in germ cells also does not suppress SG death (Yacobi-Sharon et al., 2013). These data further indicate that starvation-induced SG death is mediated by CC apoptosis.

Importantly, inhibition of CC apoptosis by DIAP1 expression did not suppress the SG death as dramatically in the eight- and 16-cell stages. Eight- and 16-cell SG death was observed even under fed conditions (Fig. 4C,D), suggesting that this class of SG death is independent of nutrient conditions. These data also imply the existence of two subclasses of SG death governed by distinct mechanisms: (1) 'early' stage death (two- and four-cell SG), which is specifically increased upon protein starvation and likely induced by CC apoptosis; and (2) 'late' stage SG death (eight- and 16-cell SG), which is observed irrespective of nutrient conditions and is less correlated with CC apoptosis. This classification is supported by the observation that CCs associated with 'early' stage SG are more frequently apoptotic during protein starvation than those associated

with 'late' stage SG (Fig. 4C,D). Consistently, dying 'early' SG are almost always accompanied by apoptotic CCs (Fig. 4E), whereas dying 'late' SG are frequently observed without accompanying apoptotic CCs (Fig. 4F). These data thus support the model in which starvation specifically increases the apoptosis of CCs associated with two-cell and four-cell SG, which in turn leads to the death of these SG (Fig. 4G).

GSC maintenance is impaired when CC-mediated SG death is inhibited during protein starvation

The highly regulated nature of CC-mediated elimination of SG compelled us to explore the biological relevance of such a response. To address this issue, we began by examining the consequence of inhibiting CC apoptosis during protein starvation. As described above, the expression of DIAP1 in the CySC/CC lineage efficiently blocks starvation-induced CC apoptosis as well as the death of associated 'early' SG (Fig. 4A,B).

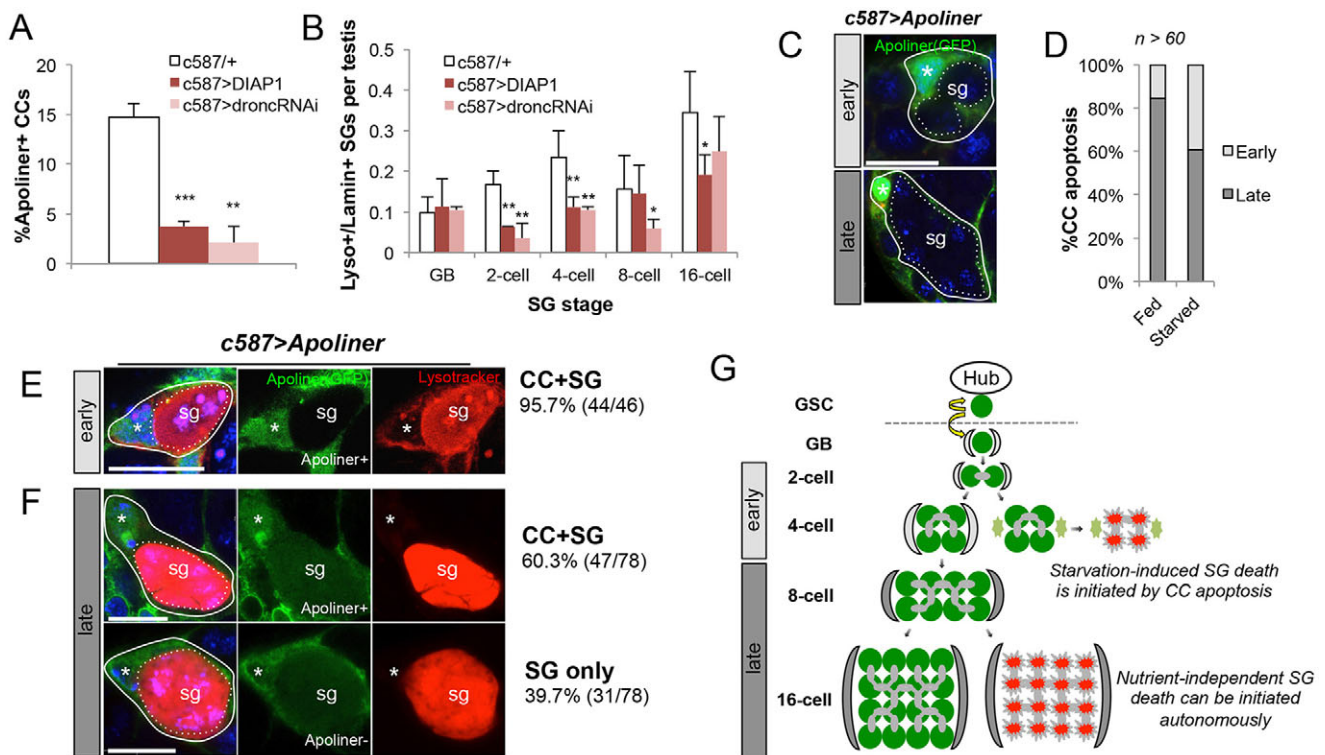


Fig. 4. CC apoptosis mediates SG death during protein starvation. (A) Quantification of CC apoptosis after 3 days of starvation with Apoliner upon overexpression of DIAP1 or Dronc RNAi knockdown. $n > 15 \times 3$ testes per data point. (B) Quantification of SG death per testis after 3 days of starvation upon overexpression of DIAP1 or Dronc RNAi knockdown. $n > 30 \times 3$ testes per data point. Data are mean \pm s.d. * $P < 0.05$; ** $P < 0.005$; *** $P < 0.0005$ (Student's *t*-test). (C) Representative images of dying CCs (solid outlines, nuclei indicated by asterisks) scored as 'early' or 'late' based on the number of enveloped SG (dotted outlines). The SG stage was determined by the number of DAPI-stained nuclei within the cyst. Scale bar: 10 μ m. (D) Percentage of 'early' and 'late' CC death in testes under fed or starved conditions (9 days). (E,F) Representative images of dying 'early' (E) and 'late' (F) SG (dotted outline) and their encapsulating CCs (solid outline, nucleus indicated by an asterisk) with observed frequencies. Whereas 'early' SG death was almost always associated with apoptotic CC (95.7%), 'late' SG death was associated with apoptotic CC for only 60.3% of the time. (G) Model: starvation-induced 'early' SG death is initiated by CC apoptosis, whereas 'late' SG death can be initiated independently of CC apoptosis.

Strikingly, we found that DIAP1-expressing testes cannot maintain GSCs at a steady state during protein starvation. Whereas wild-type/control flies maintain six actively proliferating GSCs per testis for an extended period of time during protein starvation, flies expressing DIAP1 in CySC/CC lineage (*c587>DIAP1*) continued to lose GSCs, decreasing to only ~ 3 germ cells attaching to the hub at day 12 of protein starvation (Fig. 5A). In addition to a decreased number, we found that the rate of GSC cell cycle progression is decreased in DIAP1-expressing flies during starvation (Fig. 5B, compare with Fig. 1D, day 9–11). Moreover, the remaining germ cells attaching to the hub did not appear to be normal GSCs, as they were often connected to other germ cells by a fusome and resemble SG rather than GSCs (Fig. 5C–E). After 18 days of starvation, only 31% of remaining hub-associated germ cells appear to be single-cell GSCs (18% two cell, 42% four cell, 9% eight cell, $n = 90$ hub-associated germ cells), leading to the calculation of less than one bona fide GSC per hub in starved DIAP1-expressing flies (31% \times 2.8 germ cells/hub = 0.9 GSCs). By contrast, SG-like germ cells are much less often observed attached to the hub in wild-type testes after 18 days of starvation (<10%). Importantly, DIAP1 expression did not significantly affect GSC number under fed conditions (7.6 ± 1.1 GSCs per testis, day 9, $n > 30$ testes, compared with 8.0 ± 0.5 in wild type, $P > 0.05$), nor did it alter germ cell development or testis morphology. This indicates that the blockade of CC apoptosis does not impair CySC/CC function under fed conditions but adversely affects GSC maintenance during protein starvation.

The combined loss of GSCs and reduction in GSC cell cycle led to collapse in tissue maintenance during protein starvation in DIAP1-expressing testes. First, after 9 days of starvation, we observed that SG number decreased significantly in DIAP1-expressing testes compared with control testes (supplementary material Fig. S7) despite blockade of SG death, likely due to (at least in part) decreased GSC number and cell cycle slow down (Fig. 5A,B). Moreover, after 18 days, a small but non-negligible fraction of testes lacked GSCs and other germ cells in DIAP1-expressing starved flies (5/105 testes at 18 days of starvation; 6/62 testes after 24 days of starvation) (Fig. 5F,G). These results suggest that CC-mediated SG death is crucial for maintaining functional GSCs and preserving tissue homeostasis during protein starvation.

Inhibition of CC-mediated SG death during protein starvation leads to impaired germline recovery upon reintroduction of protein

Because GSC maintenance during protein starvation is compromised in the absence of CC-mediated SG death (DIAP1-expressing testes), we wondered how germline recovery upon reintroduction of dietary protein might be affected in DIAP1-expressing testes. To assess recovery, we reintroduced protein into the diet after flies were starved for 18 days. Consistent with previously reported observations (McLeod et al., 2010), testis involution is reversible, and robust gametogenesis was efficiently reconstituted in all wild-type/control testes within 6 days of protein

reintroduction (Fig. 6A,A', 100%, $n>100$). In DIAP1-expressing testes, however, only 54% of testes were able to recover to this state within 6 days (Fig. 6B,B', $n=73$). Even after 12 days of recovery, only 60% of DIAP1-expressing testes exhibited full recovery (Fig. 6C, $n=30$).

The remaining fraction of testes (46% of testes after 6 days of recovery, $n=73$) had severely impaired recovery upon protein reintroduction. We found that 40% of DIAP1-expressing testes contained only SG, but not spermatocytes or later stage germ cells, apparently because they failed to develop to the spermatocyte stage (Fig. 6D,D'). In these cases, no spermatocytes or elongating spermatids were observed, even when recovery was extended to 12 days (Fig. 6E). Remarkably, these testes occasionally contained overproliferating SG, characterized by more than 16 SG connected by a fusome (Fig. 6F; five abnormal SG cysts/73 testes after 6 days refeeding; three abnormal SG cysts/29 testes after 12 days refeeding). Finally, the remaining 6% of testes contained no germ cells after 6 or 12 days of recovery (Fig. 6G,H), presumably representing testes that had completely lost GSCs during starvation (Fig. 5H). In these testes, protein reintroduction resulted in the overproliferation of undifferentiated CySCs (Fig. 6H'), likely due to a dysfunctional signaling environment in the absence of germ cells (Gonczy and DiNardo, 1996).

These results demonstrate that compromised CC/SG death during protein starvation leads to a collapse in tissue homeostasis, including defective GSC maintenance, which in turn severely impairs the ability of the tissue to recover. The damaged tissue architecture can also promote the abnormal overproliferation of cells during recovery.

SG death is associated with phagocytosis and JNK-pathway activation

The elimination of transit-amplifying cells could be considered to be sacrificial in nature, as it allows stem cells to be maintained. Indirectly, SG death lowers the nutrient demand of the testis and indirectly increases nutrient availability to GSCs. However, considering the fact that the flies are not fed any protein for a prolonged time period in our experimental procedure, it is unlikely that GSCs are able to maintain such an active state solely because of decreased competition for resources within the tissue. Our observations suggest that dying SG may also provide a source of nutrients that can be locally recycled. We observed that surviving CySC/CCs near dying SG/CCs become highly positive with lysosomes (Fig. 7A), possibly indicating that the contents of dying cells are transferred to surviving cells. Furthermore, these cells upregulate the JNK pathway, as monitored by expression of

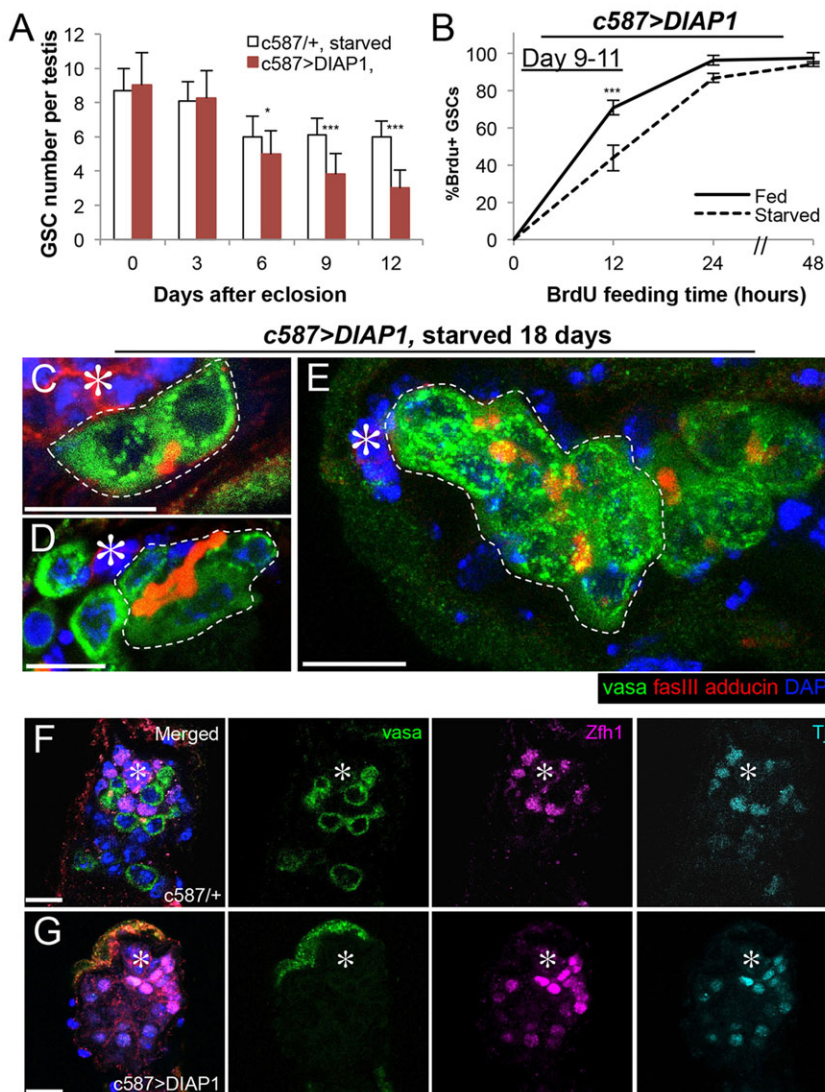


Fig. 5. GSC maintenance is impaired during protein starvation upon blockade of CC apoptosis. (A) Average GSC number per testis over 12 days of starvation in DIAP1-expressing testes (*c587>DIAP1*). Data are mean \pm s.d. $n>30$ testes per data point. * $P<0.05$; *** $P<0.0005$ (Student's *t*-test). (B) BrdU incorporation kinetics in GSCs upon overexpression of DIAP1, demonstrating cell cycle slowdown upon starvation (contrary to wild type in which GSC cell cycle is unchanged between fed and starved conditions, Fig. 1D). Data are mean \pm s.d. $n>100\times 3$ GSCs per data point. (C–E) Representative images of interconnected two-cell (C), four-cell (D) and eight-cell (E) SG-like clusters attached to the hub at 18 days of starvation in DIAP1-overexpressing testis. (F) Representative images of a control testis that contains both germ cells and CySCs/CCs after 18 days of starvation. (G) Representative images of a DIAP1-expressing testis that contains CySC/CCs but is devoid of germ cells after 18 days of starvation. In C–G, the hub is indicated with asterisks. Scale bars: 10 μ m.

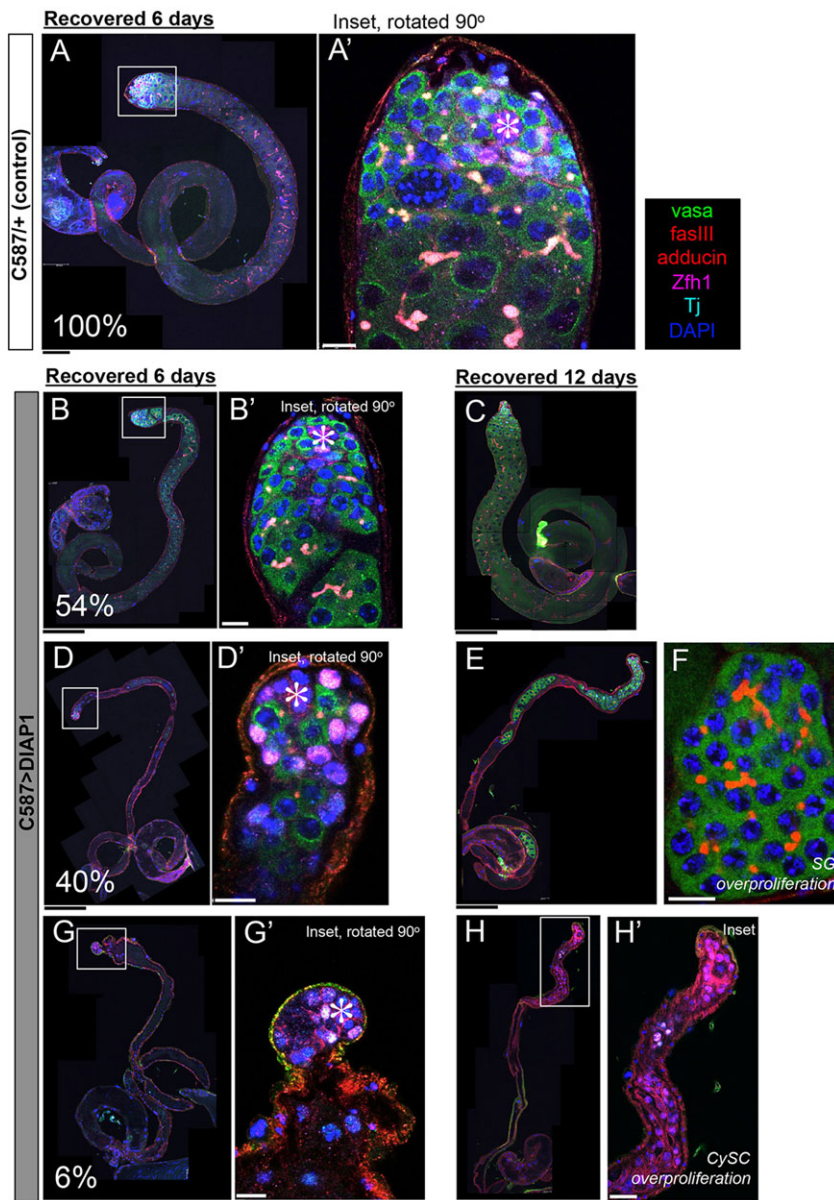


Fig. 6. Impaired recovery of spermatogenesis in DIAP1-expressing flies. *c587>DIAP1* or control flies are starved for 18 days before protein is reintroduced into the diet.

(A) Control testis with full recovery after 6 days of protein reintroduction (100%). (B,C) Only 54% of *DIAP1*-overexpressing testes reconstitute spermatogenesis after 6 days of recovery (B) or 60% after 12 days of recovery (C). (D) An example of a testis that contains only GSC, CySCs and few SG, but not spermatocytes after 6 days of recovery (40%). (E) An example of a *DIAP1*-expressing testis after 12 days of recovery, containing no spermatocytes. (F) An example of overproliferating spermatogonia in testes that lacks spermatocytes after the recovery period. (G,H) Examples of *DIAP1*-expressing testes without germ cells after 6 days (G) or 12 days (H) of protein reintroduction. After 12 days of recovery, *Zfh1*⁺ somatic cells overproliferated (H). Scale bars: 100 μ m (black); 10 μ m (white). (A',B',D',E',G',H') Higher magnification views of indicated areas in A,B,D,G,H.

puc-lacZ (Fig. 7B) similar to the non-professional phagocytic activity of follicle cells in the *Drosophila* ovary (Etchegaray et al., 2012). Phagocytosis by Sertoli cells in the mammalian testis has been also reported (Chemes, 1986). Consistent with the role of JNK pathway in mediating GSC maintenance through SG death, we found that downregulation of JNK pathway via RNAi-mediated knockdown of *Bsk* (the *Drosophila* homolog of JNK) or overexpression of a dominant-negative form of *Bsk* in CCs led to decreased SG death. It also led to defective GSC maintenance during protein starvation, without affecting CC death (Fig. 7C–E), suggesting that the JNK pathway is required to mediate CC death-dependent GSC maintenance.

We further observed that *Atg8a* localizes on the lysosomes in surviving CySC/CCs (Fig. 7F,G), suggesting that autophagy may also be involved in the clearance of dying cells (Mehta et al., 2014). Taken together, these results imply that SG elimination might contribute to GSC maintenance partly through local recycling of nutrients. Additionally, it is also possible that the lack of SG

elimination (e.g. in *DIAP1*-expressing testes) may perturb the local signaling environment, leading to GSC loss.

DISCUSSION

Tissues alternate between different states of homeostasis in order to cope with ever-changing availability of nutrients, but little is known about how different cell populations respond in a concerted manner to maximize tissue function with limited resources. Our study reveals the importance of the regulated elimination of transit-amplifying cells during protein starvation while stem cells are relatively well maintained and continue to proliferate. Considering the proposed role of transit-amplifying cells to increase cell production without increasing stem cell divisions, it is fitting that the transit-amplifying cell population is downsized to decrease overall cell output in a tissue without dramatically affecting stem cell behavior. Failure to eliminate transit-amplifying cells during starvation results in a collapse of tissue homeostasis and leads to defects in recovery upon reintroduction of nutrients. Thus, our study

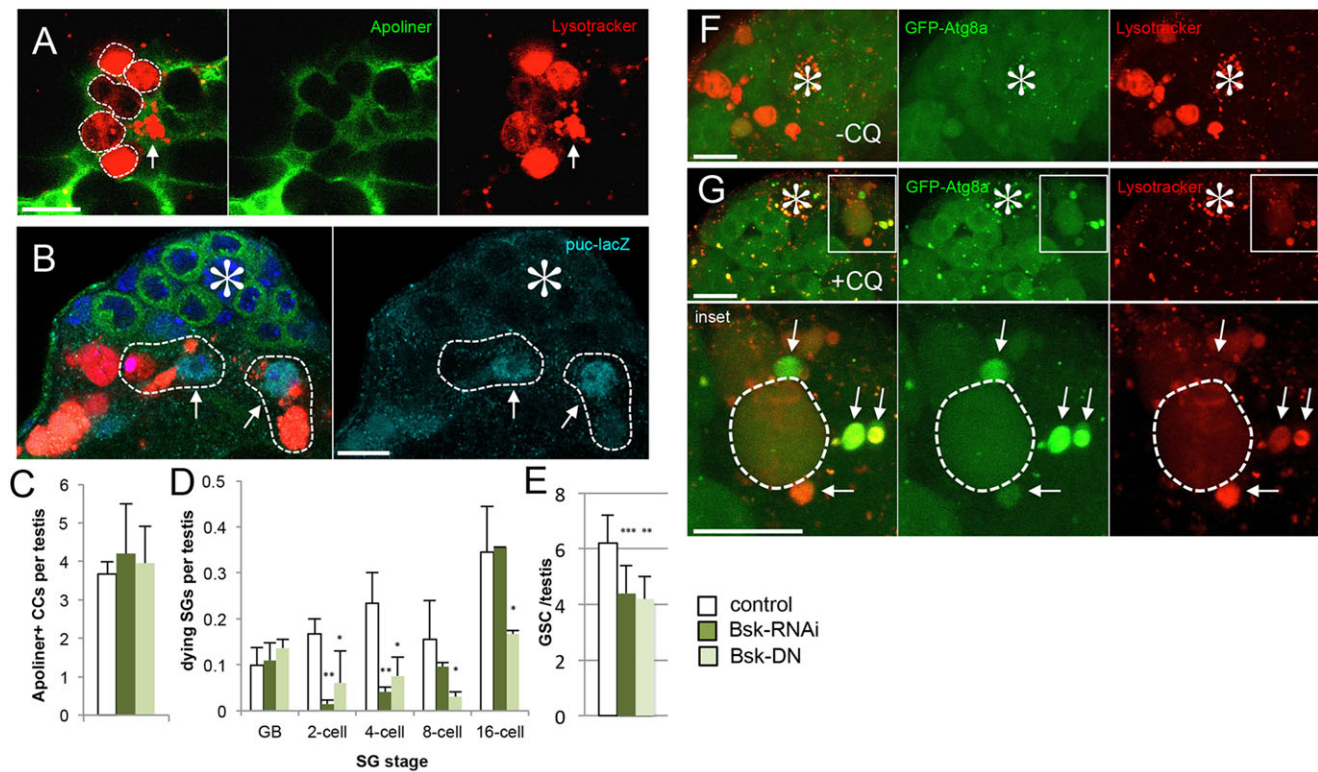


Fig. 7. Surviving CCs near the dying SG upregulate lysosome, JNK pathway and Atg8. (A) Unfixed testis stained with Lysotracker with *c587>Apoliner* as a CySC/CC marker. The Apoliner-negative, surviving CC (arrow) contains large amount of Lysosomes, when such surviving CCs are juxtaposed to dying SG (white dotted lines). (B) *puc-lacZ*⁺ CC nuclei (arrows) associated with dying SG (dotted white outlines). The hub is denoted by an asterisk. (C–E) CC apoptosis (C), SG death (D) and GSC number (E) after RNAi-mediated knockdown or expression of a dominant-negative form of Bsk. Data are mean±s.d. *n*>30 testes per data point. ****P*<0.0005, ***P*<0.005, **P*<0.05 (Student's *t*-test). (F) Without chloroquine treatment, GFP-Atg8a is observed only as scattered puncta. (G) Chloroquine treatment enhances visualization of GFP-Atg8a in lysosomes (arrows), and such GFP-Atg8a containing lysosomes (arrows) were juxtaposed to dying SG (dotted outline). Chloroquine treatment weakens Lysotracker signal, especially within dying SG. The hub is denoted by an asterisk. Lower panels are higher magnifications of the insets in the upper panels. Scale bars: 10 μm.

reveals that dramatic yet reversible ‘shifts’ in tissue homeostasis, such as the one observed during starvation, must be carried out in a precise manner that involves a coordinated response among different cell types within a tissue.

Importantly, our results do not argue that stem cells do not respond to starvation at all. We did find that stem cell divisions were transiently decreased throughout the first few days of protein starvation, similar to the ‘poor media’ response we have described previously (Roth et al., 2012), before reaching a new steady state of reduced number but active proliferation. In addition to these stem cell responses, our data highlight the importance of the dramatic response of differentiating cells in maintaining stem cells after shifting to a new steady state in the starved condition. Why this particular steady state (i.e. maintaining active GSCs while eliminating SG) is more advantageous during starvation compared with alternative states (e.g. slowed GSC proliferation) awaits future investigation.

The mechanism of GSC reduction remains elusive. Niche factors, including hub size and JAK-STAT signaling, seem unlikely to play a significant role in the decrease of GSC number from eight to six (supplementary material Fig. S1). However, we found that during protein starvation, dedifferentiation of SG was dramatically suppressed (supplementary material Fig. S8). This might be secondary to the increase in SG death, which decreases the pool of SG from which dedifferentiation occurs. Nonetheless, such a decrease in dedifferentiation may contribute to a decrease in GSC number during starvation. Our study highlights the importance of a non-autonomous role of CC death to mediate SG death during

protein starvation. It is interesting to note that the nutrient response of the soma has such a dominant role in mediating germline homeostasis, despite the well-characterized ability of the germline to sense nutrient status (Drummond-Barbosa and Spradling, 2001; McLeod et al., 2010; Roth et al., 2012; Shim et al., 2013). The nature of the crosstalk between somatic cells and germ cells that achieves concerted responses to nutrient status remains to be determined.

Finally, it is interesting to note that defective response to protein starvation due to the blockade of CC/SG cell death by DIAP1 expression leads to a tumor-like overproliferation of cells upon reintroduction of protein. These cells are not inherently tumorigenic in the classical sense, as they likely do not contain mutations in tumor suppressor genes or oncogenes. Instead, their dysregulated behavior appears to be a result of damaged tissue architecture and an imbalance among different but interdependent cell types. When these cells are exposed to nutrients again, uncontrolled proliferation and abnormal differentiation may be the consequence of an inappropriate signaling environment. By extension of this idea, it is tempting to speculate that human cells with ‘wild-type’ genomes may be triggered to form tumor in a similar manner: instead of mutations that cause these cells to be overproliferative, their tumorigenic behavior might arise from impaired tissue environment acquired during a defective ‘shift’ in tissue homeostasis. Treatment of such tumors would require fundamentally different approaches.

In summary, our study reveals regulated elimination of transit-amplifying cells as a crucial step to protect stem cells in response to starvation. We show that inhibiting this process can lead to

irreversible tissue damage, thus introducing the idea that organisms and their tissues have highly evolved strategies to undergo reversible ‘shifts’ in tissue homeostasis throughout their lifespans.

MATERIALS AND METHODS

Fly strains and husbandry

Flies were cultured in standard Bloomington medium at 25°C. For protein starvation experiments, newly eclosed adult flies were transferred within 24 h (day 0) onto either standard food (fed) or 16% sucrose/0.7% agar (starved) at a density of 20–40 flies per vial. Flies were transferred to fresh vials every 3 days. The following fly stocks were used: yw (wild type), c587-gal4 (Decotto and Spradling, 2005), nos-gal4 (Van Doren et al., 1998), UAS-Apoliner (Bloomington Stock Center), UAS-DIAP1 (Bloomington Stock Center), UAS-Dronc-RNAi (KK100424) (Vienna *Drosophila* RNAi Center), UAS-Grim (D. Bennett, University of Liverpool, UK), tub-gal80^{ts} (Bloomington Stock Center), GFP-Atg8a (E. H. Baehrecke, University of Massachusetts Medical School, Worcester, MA, USA) (Denton et al., 2009) and lacZ^{puc-A251.1} (Martin-Blanco et al., 1998).

Immunofluorescence staining and microscopy

Immunofluorescence staining of testes was performed as described previously (Cheng et al., 2008). Briefly, testes were dissected in PBS, transferred to 4% formaldehyde in PBS and fixed for 30–60 min. The testes were then washed in PBS-T (PBS containing 0.1% Triton-X) for at least 30 min, followed by incubation with primary antibody in 3% bovine serum albumin (BSA) in PBS-T at 4°C overnight. Samples were washed for 60 min (three 20 min washes) in PBS-T, incubated with secondary antibody in 3% BSA in PBS-T at 4°C overnight, washed as above, and mounted in VECTASHIELD with DAPI (Vector Labs). The following primary antibodies were used: mouse anti-Adducin-like (hu li tai shao – Fly Base) [1:20; Developmental Studies Hybridoma Bank (DSHB); developed by H. D. Lipshitz (University of Toronto, Canada)] (Ding et al., 1993); rat anti-Vasa (1:50; DSHB; developed by A. Spradling, Carnegie Institution for Science, Baltimore, MD, USA), rabbit anti-Vasa (1:200; d-26; Santa Cruz Biotechnology) (Roth et al., 2012), mouse anti-Fasciclin III (1:200; DSHB; developed by C. Goodman, UCSF, CA, USA) (Patel et al., 1987), mouse anti-Lamin Dm0 (1:200; DSHB; developed by P. A. Fisher, Stony Brook University School of Medicine, NY, USA) (Klapper et al., 1997), rabbit anti-Thr3-phosphorylated Histone H3 (PH3) (1:200; Upstate, Millipore); rat anti-BrdU [1:100, BU1/75 (ICR1); Abcam] (Takashima et al., 2008), guinea pig anti-Traffic jam (Tj) (1:400; a kind gift from Dorothea Godt, University of Toronto, Canada) (Li et al., 2003), rabbit anti-Zfh1 (1:5000; a kind gift from Ruth Lehmann, NYU School of Medicine, NY, USA) (Broihier et al., 1998) and rabbit anti-cleaved caspase 3 (1:400; Cell Signaling Technology) (Di Cunto et al., 2000). Images were taken using Leica TCS SP5 and TCS SP8 confocal microscopes with a 63× oil-immersion objective (NA=1.4) and processed using Adobe Photoshop software.

For observation of unfixed testes, testes were mounted onto slides with PBS and imaged within 10 min of dissection to minimize the effects of hypoxia. LysoTracker was used to label lysosomes and dying germ cells. For visualization of GFP-Atg8a, flies were fed 1 mM chloroquine (Sigma) for 12 h prior to dissection.

Cell cycle analysis

For BrdU feeding assay, previously fed or starved adult flies were transferred into fresh vials of food or starvation media containing BrdU (1 mg/ml). Methylene Blue was also added to the media to monitor feeding behavior. Testes were dissected and analyzed at 12, 24 and 48 h after initiation of BrdU feeding. For *ex vivo* S-phase analysis, testes were soaked in PBS with BrdU (0.1 mg/ml) for 45 min prior to fixation. Testes from both BrdU experiments were then treated with RQ1 DNase in 1× DNase buffer (Promega) for 2 h and incubated with primary antibody (anti-BrdU and anti-vasa) overnight at 4°C. For mitotic index analysis, testes were dissected and fixed within 5 min of anesthesia to minimize effects of elevated CO₂ on mitoses (Inaba et al., 2011). Testes were then stained with anti-PH3 and processed as described above.

Quantification of cell death

For detection of germ cell death, testes were stained with LysoTracker Red DND-99 (Life Technologies) in PBS for 30 min prior to formaldehyde fixation. Anti-lamin Dm0 staining (described above) was used to outline intact nuclear envelope. Dying SG were scored according to stage by counting the number of LysoTracker⁺ and lamin⁺ germ cell nuclei within a cyst (supplementary material Fig. S4B,C). Dying SG that lacked lamin staining, likely reflecting nuclear disintegration during later stages of germ cell death, were excluded from our scoring. Occasionally, dying SG had irregular numbers of countable germ cells (e.g. 3, 6, 12); these were included in our data by rounding up to the nearest power of two (4, 8, 16).

Acknowledgements

We thank Dorothea Godt, Ruth Lehmann, Margaret Fuller, Charlie Kuang, Cheng-Yu Lee, Bloomington Stock Center and Developmental Studies Hybridoma Bank for reagents, and Yamashita lab members for discussions and comments on the manuscript.

Competing interests

The authors declare no competing or financial interests.

Author contributions

H.Y. designed and conducted experiments. H.Y. and Y.M.Y. interpreted the results, wrote and edited the manuscript.

Funding

This work was supported the University of Michigan Medical Scientist Training Program, by a training grant from the University of Michigan Program in Cellular and Molecular Biology [T32 GM007315] and by a National Institutes of Health (NIH) Fellowship [F30 AG045021-01] to H.Y. The research in Yamashita's laboratory is supported by the Howard Hughes Medical Institute. Y.M.Y. is supported by the MacArthur Foundation. Deposited in PMC for release after 6 months.

Supplementary material

Supplementary material available online at <http://dev.biologists.org/lookup/suppl/doi:10.1242/dev.122663/-/DC1>

References

- Angelo, G. and Van Gilst, M. R. (2009). Starvation protects germline stem cells and extends reproductive longevity in *C. elegans*. *Science* **326**, 954–958.
- Bardet, P.-L., Kolahgar, G., Mynett, A., Miguel-Aliaga, I., Briscoe, J., Meier, P. and Vincent, J.-P. (2008). A fluorescent reporter of caspase activity for live imaging. *Proc. Natl. Acad. Sci. USA* **105**, 13901–13905.
- Broihier, H. T., Moore, L. A., Van Doren, M., Newman, S. and Lehmann, R. (1998). zfh-1 is required for germ cell migration and gonadal mesoderm development in *Drosophila*. *Development* **125**, 655–666.
- Chemes, H. (1986). The phagocytic function of Sertoli cells: a morphological, biochemical, and endocrinological study of lysosomes and acid phosphatase localization in the rat testis. *Endocrinology* **119**, 1673–1681.
- Cheng, J., Türkel, N., Hemati, N., Fuller, M. T., Hunt, A. J. and Yamashita, Y. M. (2008). Centrosome misorientation reduces stem cell division during ageing. *Nature* **456**, 599–604.
- Cheng, J., Tiyaabonchai, A., Yamashita, Y. M. and Hunt, A. J. (2011). Asymmetric division of cyst stem cells in *Drosophila* testis is ensured by anaphase spindle repositioning. *Development* **138**, 831–837.
- Davies, E. L. and Fuller, M. T. (2008). Regulation of self-renewal and differentiation in adult stem cell lineages: lessons from the *Drosophila* male germ line. *Cold Spring Harb. Symp. Quant. Biol.* **73**, 137–145.
- de Cuevas, M. and Matunis, E. L. (2011). The stem cell niche: lessons from the *Drosophila* testis. *Development* **138**, 2861–2869.
- Decotto, E. and Spradling, A. C. (2005). The *Drosophila* ovarian and testis stem cell niches: similar somatic stem cells and signals. *Dev. Cell* **9**, 501–510.
- Denton, D., Shravage, B., Simin, R., Mills, K., Berry, D. L., Baehrecke, E. H. and Kumar, S. (2009). Autophagy, not apoptosis, is essential for midgut cell death in *Drosophila*. *Curr. Biol.* **19**, 1741–1746.
- Di Cunto, F., Imarisco, S., Hirsch, E., Broccoli, V., Bulfone, A., Migheli, A., Atzori, C., Turco, E., Triolo, R., Dotto, G. P. et al. (2000). Defective neurogenesis in citron kinase knockout mice by altered cytokinesis and massive apoptosis. *Neuron* **28**, 115–127.
- Ding, D., Parkhurst, S. M. and Lipshitz, H. D. (1993). Different genetic requirements for anterior RNA localization revealed by the distribution of Adducin-like transcripts during *Drosophila* oogenesis. *Proc. Natl. Acad. Sci. USA* **90**, 2512–2516.

- Drummond-Barbosa, D. and Spradling, A. C.** (2001). Stem cells and their progeny respond to nutritional changes during *Drosophila* oogenesis. *Dev. Biol.* **231**, 265-278.
- Etchegaray, J. I., Timmons, A. K., Klein, A. P., Pritchett, T. L., Welch, E., Meehan, T. L., Li, C. and McCall, K.** (2012). Draper acts through the JNK pathway to control synchronous engulfment of dying germline cells by follicular epithelial cells. *Development* **139**, 4029-4039.
- Fielenbach, N. and Antebi, A.** (2008). *C. elegans* dauer formation and the molecular basis of plasticity. *Genes Dev.* **22**, 2149-2165.
- Gonczy, P. and DiNardo, S.** (1996). The germ line regulates somatic cyst cell proliferation and fate during *Drosophila* spermatogenesis. *Development* **122**, 2437-2447.
- Hétié, P., de Cuevas, M. and Matunis, E.** (2014). Conversion of quiescent niche cells to somatic stem cells causes ectopic niche formation in the *Drosophila* testis. *Cell Rep.* **7**, 715-721.
- Inaba, M., Yuan, H. and Yamashita, Y. M.** (2011). String (Cdc25) regulates stem cell maintenance, proliferation and aging in *Drosophila* testis. *Development* **138**, 5079-5086.
- Klapper, M., Exner, K., Kempf, A., Gehrig, C., Stuurman, N., Fisher, P. A. and Krohne, G.** (1997). Assembly of A- and B-type lamins studied in vivo with the baculovirus system. *J. Cell Sci.* **110**, 2519-2532.
- Leatherman, J. L. and DiNardo, S.** (2008). Zfh-1 controls somatic stem cell self-renewal in the *Drosophila* testis and nonautonomously influences germline stem cell self-renewal. *Cell Stem Cell* **3**, 44-54.
- Leatherman, J. L. and DiNardo, S.** (2010). Germline self-renewal requires cyst stem cells and stat regulates niche adhesion in *Drosophila* testes. *Nat. Cell Biol.* **12**, 806-811.
- Lehmann, R.** (2012). Germline stem cells: origin and destiny. *Cell Stem Cell* **10**, 729-739.
- Leulier, F., Ribeiro, P. S., Palmer, E., Tenev, T., Takahashi, K., Robertson, D., Zachariou, A., Pichaud, F., Ueda, R. and Meier, P.** (2006). Systematic in vivo RNAi analysis of putative components of the *Drosophila* cell death machinery. *Cell Death Differ.* **13**, 1663-1674.
- Li, M. A., Alls, J. D., Avancini, R. M., Koo, K. and Godt, D.** (2003). The large Maf factor Traffic Jam controls gonad morphogenesis in *Drosophila*. *Nat. Cell Biol.* **5**, 994-1000.
- Lim, J. G. Y. and Fuller, M. T.** (2012). Somatic cell lineage is required for differentiation and not maintenance of germline stem cells in *Drosophila* testes. *Proc. Natl. Acad. Sci. USA* **109**, 18477-18481.
- Lin, H., Yue, L. and Spradling, A. C.** (1994). The *Drosophila* fusome, a germline-specific organelle, contains membrane skeletal proteins and functions in cyst formation. *Development* **120**, 947-956.
- Lopes, F. L., Desmarais, J. A. and Murphy, B. D.** (2004). Embryonic diapause and its regulation. *Reproduction* **128**, 669-678.
- Losick, V. P., Morris, L. X., Fox, D. T. and Spradling, A.** (2011). *Drosophila* stem cell niches: a decade of discovery suggests a unified view of stem cell regulation. *Dev. Cell* **21**, 159-171.
- Lui, J. H., Hansen, D. V. and Kriegstein, A. R.** (2011). Development and evolution of the human neocortex. *Cell* **146**, 18-36.
- Martin-Blanco, E., Gampel, A., Ring, J., Virdee, K., Kirov, N., Tolkovsky, A. M. and Martinez-Arias, A.** (1998). puckered encodes a phosphatase that mediates a feedback loop regulating JNK activity during dorsal closure in *Drosophila*. *Genes Dev.* **12**, 557-570.
- McLeod, C. J., Wang, L., Wong, C. and Jones, D. L.** (2010). Stem cell dynamics in response to nutrient availability. *Curr. Biol.* **20**, 2100-2105.
- Mehta, P., Henault, J., Kolbeck, R. and Sanjuan, M. A.** (2014). Noncanonical autophagy: one small step for LC3, one giant leap for immunity. *Curr. Opin. Immunol.* **26**, 69-75.
- Mihaylova, M. M., Sabatini, D. M. and Yilmaz, O. H.** (2014). Dietary and metabolic control of stem cell function in physiology and cancer. *Cell Stem Cell* **14**, 292-305.
- Nakada, D., Levi, B. P. and Morrison, S. J.** (2011). Integrating physiological regulation with stem cell and tissue homeostasis. *Neuron* **70**, 703-718.
- Orme, M. and Meier, P.** (2009). Inhibitor of apoptosis proteins in *Drosophila*: gatekeepers of death. *Apoptosis* **14**, 950-960.
- Padilla, P. A. and Ladage, M. L.** (2012). Suspended animation, diapause and quiescence: arresting the cell cycle in *C. elegans*. *Cell Cycle* **11**, 1672-1679.
- Patel, N. H., Snow, P. M. and Goodman, C. S.** (1987). Characterization and cloning of fasciclin III: a glycoprotein expressed on a subset of neurons and axon pathways in *Drosophila*. *Cell* **48**, 975-988.
- Roth, T. M., Chiang, C.-Y. A., Inaba, M., Yuan, H., Salzman, V., Roth, C. E. and Yamashita, Y. M.** (2012). Centrosome misorientation mediates slowing of the cell cycle under limited nutrient conditions in *Drosophila* male germline stem cells. *Mol. Biol. Cell* **23**, 1524-1532.
- Schulz, C., Wood, C. G., Jones, D. L., Tazuke, S. I. and Fuller, M. T.** (2002). Signaling from germ cells mediated by the rhomboid homolog stet organizes encapsulation by somatic support cells. *Development* **129**, 4523-4534.
- Shim, J., Gururaja-Rao, S. and Banerjee, U.** (2013). Nutritional regulation of stem and progenitor cells in *Drosophila*. *Development* **140**, 4647-4656.
- Takashima, S., Mkrtychyan, M., Younossi-Hartenstein, A., Merriam, J. R. and Hartenstein, V.** (2008). The behaviour of *Drosophila* adult hindgut stem cells is controlled by Wnt and Hh signalling. *Nature* **454**, 651-655.
- Tatar, M. and Yin, C.-M.** (2001). Slow aging during insect reproductive diapause: why butterflies, grasshoppers and flies are like worms. *Exp. Gerontol.* **36**, 723-738.
- Tazuke, S. I., Schulz, C., Gilboa, L., Fogarty, M., Mahowald, A. P., Guichet, A., Ephrussi, A., Wood, C. G., Lehmann, R. and Fuller, M. T.** (2002). A germline-specific gap junction protein required for survival of differentiating early germ cells. *Development* **129**, 2529-2539.
- van der Flier, L. G. and Clevers, H.** (2009). Stem cells, self-renewal, and differentiation in the intestinal epithelium. *Annu. Rev. Physiol.* **71**, 241-260.
- Van Doren, M., Williamson, A. L. and Lehmann, R.** (1998). Regulation of zygotic gene expression in *Drosophila* primordial germ cells. *Curr. Biol.* **8**, 243-246.
- Wang, L., McLeod, C. J. and Jones, D. L.** (2011). Regulation of adult stem cell behavior by nutrient signaling. *Cell Cycle* **10**, 2628-2634.
- Watt, F. M.** (1998). Epidermal stem cells: markers, patterning and the control of stem cell fate. *Philos. Trans. R. Soc. Lond. B Biol. Sci.* **353**, 831-837.
- Yacobi-Sharon, K., Namdar, Y. and Arama, E.** (2013). Alternative germ cell death pathway in *Drosophila* involves HtrA2/Omi, lysosomes, and a caspase-9 counterpart. *Dev. Cell* **25**, 29-42.
- Yilmaz, Ö. H., Katajisto, P., Lamming, D. W., Gültekin, Y., Bauer-Rowe, K. E., Sengupta, S., Birsoy, K., Dursun, A., Yilmaz, V. O., Selig, M. et al.** (2012). mTORC1 in the Paneth cell niche couples intestinal stem-cell function to calorie intake. *Nature* **486**, 490-495.